PREPRINTS

OF THE

STEWARD OBSERVATORY

THE UNIVERSITY OF ARIZONA
TUCSON, ARIZONA

NO. 37

EVOLUTION IN GALAXY NUCLEI I,

COMPARISON OF THE COMA AND VIRGO CLUSTERS

by

William G. Tifft

Steward Observatory
University of Arizona
Tucson, Arizona

Submitted March 1971

EVOLUTION IN GALAXY NUCLEI I,

COMPARISON OF THE COMA AND VIRGO CLUSTERS

William G. Tifft

Steward Observatory

University of Arizona

Received March 1971

ABSTRACT

The correlation of nuclear magnitude with redshift in the Coma and Virgo Clusters is discussed. The two clusters are combined in a fitting process to determine a differential distance modulus of 3.47 ±0.05. Hubble velocities of the clusters are found to be 1284 ±45 and 6344 ±70. For a Virgo Cluster distance of 14.8 Mpc the Hubble constant is H = 86.3 ±3, subject to the usual major systematic errors. The effect of the redshift-magnitude correlation on the luminosity functions of the Coma and Virgo Cluster is discussed and can account for observed nonuniformity in the luminosity functions.

The observed redshift distribution within clusters is interpreted as a uniform Hubble velocity upon which is superimposed a differential redshift not due to mass center motion. A combination of gravitational redshifts and radial mass motion induced in an evolving nuclear gravitational potential field is suggested to produce the differential redshifts. Galaxies are viewed as expanding systems evolving from dense cores with the redshift-magnitude correlation representing a form of evolutionary track. Clusters as a whole can be dynamically stable. The outflow of material is a source of intergalactic bridges, intergalactic stellar haze, and various phenomena observed in galaxy envelopes. The concept of evolving galaxies has major consequences on cosmological models. Age dispersion in clusters and possible evolutionary corrections to galaxy redshifts and total luminosities both suggest that a new approach to a steady state concept is possible.

INTRODUCTION

A non-random correlation between redshift and nuclear magnitudes for bright galaxies in the Virgo Cluster was indicated to be present by Tifft (1970). An early form of the concept may be ascribed to Holmberg (1961). Tifft (1970) has given a tentative interpretation in terms of nuclear-driven evolution of galaxies. Holmberg (1961) attempted to use such an effect to introduce systematic corrections into redshift determinations. DeVaucouleurs and deVaucouleurs (1963) have, however, shown that systematic errors arising from nuclear magnitude effects are not important. This paper, subsequently referred to as EGN I, extends the observations made in the Virgo Cluster to the Coma Cluster, combines the data by a fitting process to provide a new means of calibration of the Hubble parameter, and discusses potential applications and implications of the redshift magnitude correlation and galaxian evolutionary concept.

THE VIRGO CLUSTER

Table I is a tabulation of redshift, V magnitude through five successive apertures, and membership in subsystems of the Virgo Cluster. The list is limited to membership in the E and S subsystems defined by deVaucouleurs (1961b) to retain maximum homogeneity of the sample. The sample is complete to magnitude 12.0 in the Shapley-Ames catalog. The photometry has been derived from four color photoelectric observations by Tifft (1969) transformed according to the equation

$$V = 0.25 + (3) - (3\text{-}4) + 0.265\ (2\text{-}3). \qquad (1)$$

Equation (1) is a combination of transformations given by deVaucouleurs (1961a). Redshifts have been taken from the Reference Catalog of Bright Galaxies (deVaucouleurs and deVaucouleurs, 1964) or more recent measurements by

TABLE I -- VIRGO CLUSTER GALAXIES

NGC	REDSHIFT*	$V_{9.7}$	$V_{16.1}$	$V_{25.8}$	$V_{38.7}$	$V_{64.5}$	TYPE**	SYSTEM
4192	- 199	13.65	13.14	12.62	12.15	11.60	Sb	S
4216	- 43	12.65	12.07	11.61	11.29	10.95	Sb	S
4254	2397	13.89	13.13	12.34	11.77	11.14	Sc	S
4293	695	14.45	13.75	13.00	12.42	11.82	Sa	E
4321	1552	13.48	12.70	12.11	11.77	11.35	Sc	S
4374	878	12.30	11.63	11.09	10.72	10.33	SO	E
4382	712	12.18	11.65	11.18	10.81	10.38	SO	E
4406	- 367	12.56	11.97	11.41	11.00	10.55	E3	E
4421	1628	14.05	13.51	13.06	12.69	12.19	SBa	S
4429	1032	13.02	12.51	11.90	11.47	10.98	SO	E
4435	796	13.25	12.74	12.33	12.04	11.72	SBO	E
4438	- 105	13.40	12.79	12.15	11.66	11.22	Sap	E
4442	493	12.51	11.97	11.51	11.23	10.92	SBO	E
4450	1992	13.19	12.66	12.11	11.70	11.22	Sb	S?
4459	1042	12.87	12.35	11.81	11.44	11.04	SO	E
4472	855	12.16	11.47	10.88	10.43	9.93	E1	E
4473	2171	12.37	11.84	11.47	11.19	10.89	E5	E
4477	1194	12.98	12.41	11.92	11.58	11.21	SBO	E
4486	1187	12.69	11.90	11.19	10.69	10.17	EO	E
4501	2056	13.17	12.58	12.00	11.52	10.90	Sc	S
4526	396	12.51	11.91	11.35	10.95	10.50	SO	E
4548	371	13.55	13.01	12.46	12.04	11.45	SBb	S
4550	279	13.54	12.93	12.41	12.11	11.87	E7	E
4552	195	12.27	11.72	11.30	11.00	10.65	EO	E
4569	- 300	12.58	12.22	11.86	11.56	11.09	Sb	S
4579	1680	12.64	12.06	11.59	11.21	10.80	Sb	S
4621	345	12.37	11.89	11.41	11.08	10.68	E5	E
4649	1200	12.24	11.54	10.94	10.53	10.10	E2	E
4651	685	13.78	13.17	12.52	12.00	11.42	--	S?
4654	960	14.61	14.03	13.27	12.63	11.86	Sc	S
4762	876	12.81	12.35	11.90	11.60	11.18	Sa	E?

* Corrected for galactic rotation.
** Humason, Mayall, and Sandage (1956).

deVaucouleurs and deVaucouleurs (1967). One exception to this is NGC 4569 where the nuclear redshift given by Rodgers and Freeman (1970) is listed.

Figure 1 is a plot of 9.7 arc second photometry against redshift and constitutes the primary original evidence for the redshift-nuclear magnitude correlation referred to the UBV system of photometry. The upper part of Figure 1 contains E, SO, SBO, and some Sa type galaxies while the lower part contains later spiral types. One of the spirals, NGC 4293, was classified in the E subsystem by deVaucouleurs (1961b) but it behaves photometrically like the S types. This galaxy is a spiral as may be seen from the photograph in The Hubble Atlas of Galaxies (Sandage, 1961). The notations n-branch, rp-branch, and S-region are retained as originally defined (Tifft, 1970). The transitional loop, joining the two main branches at the low redshift end, will be denoted as the transitional or T-region. The elliptical-like galaxies, including SO types, define the primary branches of the correlation. Sprials include some which parallel the elliptical behavior (primarily Sb types) and some which fall below the main structure in the diagrams and define the S region (primarily Sc types).

Figure 2 is the same as Figure 1 except 38.7 arc second photometry has been plotted. The correlation remains visible but scatter increases as more outer structural features influence the photometry and dilute the nuclear effects. Spiral galaxies which are well separated from ellipticals at 9.7 arc seconds tend to converge toward the ellipticals at 38.7 arc seconds. NGC 4486, which falls at the tip of the n-branch at 38.7 arc seconds, shows a tendency to become rapidly fainter at 9.7 arc seconds. There is a general tendency for nuclei to become more diffuse as one progresses along the n-branch toward higher redshifts (Tifft, 1970). Thus, at small apertures the entire n-branch turns back toward the rp-branch and extremely diffuse nuclei as in

FIGURE 1

9.7 second of arc nuclear V photometry of bright galaxies.in the Virgo Cluster as a function of redshift. The relationship defined by the E galaxies is reproduced in the lower part of the figure where S galaxies are plotted.

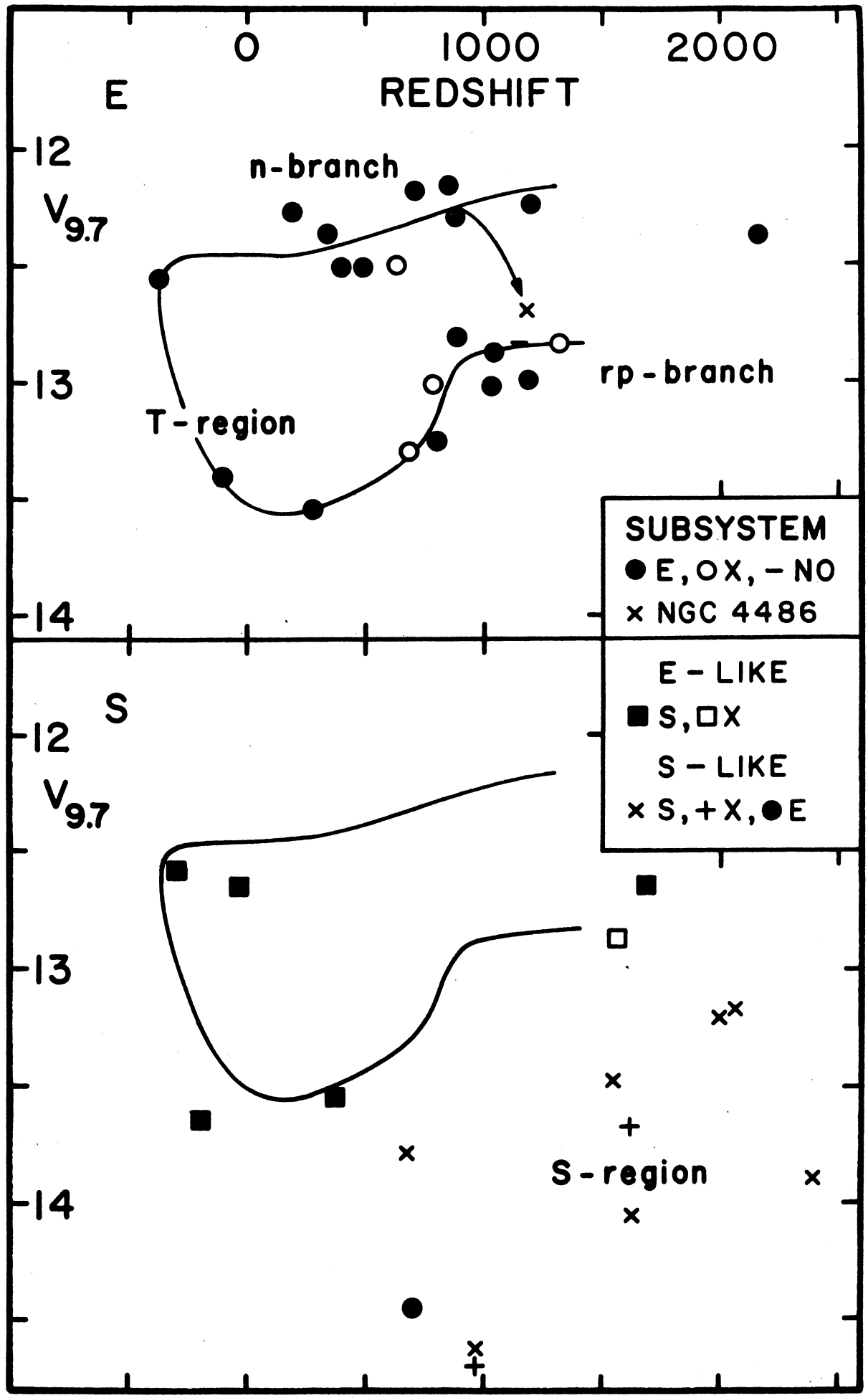
0
1000
2000
REDSHIFT
E
12
$V_{9.7}$
n-branch
13
T-region
rp-branch
14
SUBSYSTEM
● E, ○ X, – NO
× NGC 4486
E-LIKE
■ S, □ X
S-LIKE
× S, + X, ● E
S
12
$V_{9.7}$
13
S-region
14

FIGURE 2

38.7 second of arc nuclear V photometry of bright galaxies in the Virgo Cluster as a function of redshift. In comparison with Figure 1 the n-branch is considerably steeper and the higher redshift galaxies are more directly in line with the E galaxy relationship.

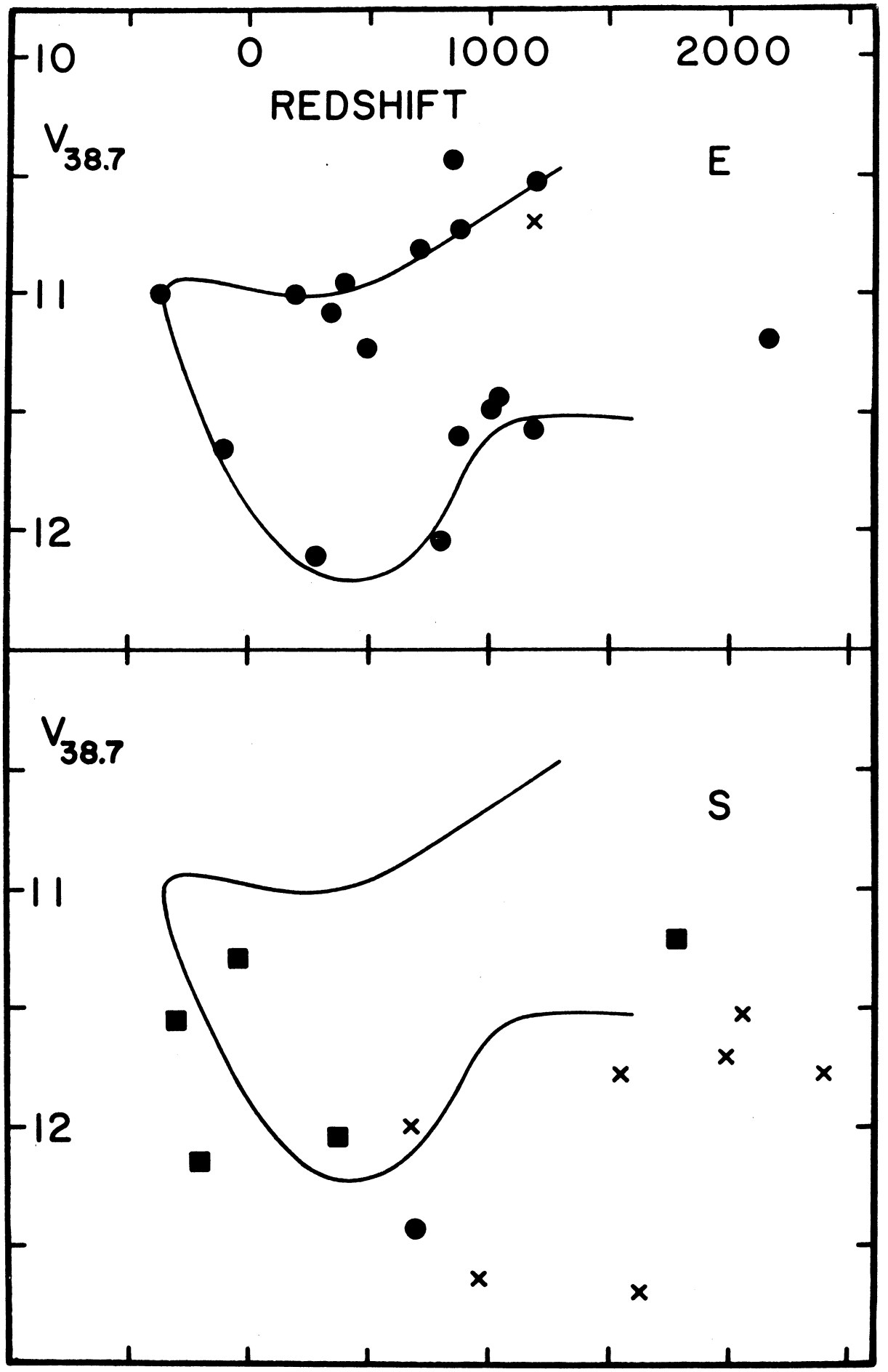
10
0
1000
2000
REDSHIFT
V38.7
E
11
12
V38.7
S
11
12

NGC 4486 may actually drop below. The correlation has been extended to integrated magnitudes (EGN II, in preparation) and confirms the tendencies for change in the V-m correlation with aperture.

At the present time data outside the core regions of clusters of galaxies is limited and inhomogeneous. The luminosity function apparently varies with radius in the Coma Cluster (Rood, 1969) and may indicate a relaxation condition with more massive objects centrally concentrated. DeVaucouleurs (1961b) assigns most of the outlying or "southern extension" galaxies in the Virgo region to a distinct subsystem denoted X, and which is in turn subdivided into northwestern and southeastern portions. Kowal (1969) has offered evidence from supernovae that the X, S, and E and some smaller "background" subgroupings are parts of one equidistant complex. The E and S subsystems have the same center and in view of this paper which ascribes to galaxy nuclei appreciable redshifts not due to mass center motion, the E and S clouds are here assumed to be spatially coincident. Figure 1 includes seven available outlying galaxies belonging to the X subsystem and NGC 4179 which is not assigned to any subsystem. They are entirely coincident with the E group; however, there are differences in the degree of nuclear light concentration and the fit to the E subsystem deviates at larger apertures; this effect is discussed in detail in EGN II (in preparation). The discussion in this paper is limited to the central regions of clusters to avoid radial variation effects.

THE COMA CLUSTER

Detailed V photometry of galaxies in the Coma Cluster has been carried out by Rood and Baum (1967, 1968). A large number of redshift measurements, in addition to those contained in the Humason, Mayall, and Sandage (1956) redshift catalog, are now available from Rood, et. al. (1971). Thirteen

additional redshifts have been determined by the author using the image tube spectrograph attached to the Steward Observatory 90-inch reflector at Kitt Peak. The photometry by Rood and Baum provides magnitude V(A) within elliptical isophotes of semi-major axis A. For all galaxies, this photometry has been converted to magnitudes V(R) within circular apertures in order to compare with the Virgo circular aperture photometry. The correction procedure followed is contained in an appendix to the calibration paper by Rood and Baum (1968). This simple correction procedure cannot be accurately applied to SBO galaxies which do not have strictly elliptical isophotes, hence, magnitueds for these galaxies are more uncertain. Table II contains a complete summary of redshifts and circular aperture magnitudes in six steps from 4.80 to 12.05 arc seconds. All E, SO, SBO and SBa galaxies in the Coma core with $V(4''.80) \leq 16.0$ and some fainter are included. All have redshifts; a program is in progress to complete redshifts to still fainter limits.

Figure 3 presents the redshift-magnitude diagram, henceforth called the V-m diagram for 5.22 arc second interpolated photometry of E, SO, and SBO galaxies in the Coma Cluster. Two galaxies with uncertain redshifts, and one with discordant photometry are omitted. The same figure contains the Virgo Cluster diagram for 25.8 arc second measurements. At the relative distances of the two clusters, 4.94 as derived in the following section, the two diagrams are equivalent. Both clusters contain a population falling on the rp-branch and in the T-region. The Coma Cluster rp-branch extends to higher redshifts, but in the overlap region the diagrams are identical. The transition from the rp-branch into the T-region appears to occur at lower redshifts for SO galaxies compared to E or SBO types as shown by the dashed lines. The same effect is seen in both clusters. The E galaxies defining the Coma rp-branch form a remarkably homogeneous group. The Coma S

TABLE II -- COMA CLUSTER V(R) AND OTHER DATA

IDENTITY	REDSHIFT	m(4.80)	m(5.64)	m(6.47)	m(7.96)	m(9.57)	m(12.05)
			E GALAXIES				
R 241	7254	15.61	15.47	15.35	15.18	15.05	14.92
I 3957	(6437)	15.91	15.79	15.70	15.56	15.46	15.36
I 3959	6968	15.43	15.32	15.21	15.05	14.94	14.82
N 4864	6831	15.46	15.28	15.14	14.92	14.76	14.60
N 4867	4827	15.49	15.34	15.23	15.08	14.96	14.86
R 223	6879	17.06	16.97	16.89	16.81	16.75	16.70
N 4865	4655	15.07	14.90	14.74	14.54	14.40	14.26
N 4869	6715	15.41	15.23	15.09	14.89	14.75	14.58
I 3976	6937	15.40	15.27	15.18	15.07	14.97	14.89
N 4876	6979	15.61	15.47	15.33	15.16	15.03	14.89
N 4881	6705	15.51	15.31	15.18	14.98	14.84	14.65
N 4886	6227	15.82	15.61	1 .48	15.27	15.10	14.93
N 4889	6456	14.54	14.35	14.14	13.90	13.71	13.54
I 4012	7232	15.68	15.56	15.45	15.32	15.22	15.14
R 167	6771	16.05	15.92	15.81	15.64	15.52	15.42
I 4021	5802	15.95	15.79	15.69	15.53	15.44	15.32
N 4898	6948	15.22	15.06	14.94	14.75	14.60	14.44
N 4906	7588	15.92	15.74	15.60	15.36	15.19	15.03
N 4908	8851	15.48	15.30	15.17	14.97	14.82	14.66
I 4045	6541	15.40	15.23	15.09	14.91	14.77	14.63
I 4051	4945	15.76	15.57	15.40	15.14	14.96	14.74
			SO GALAXIES				
N 4850	5995	15.53	15.38	15.26	15.07	14.95	14.80
I 3946	6112	15.29	15.16	15.03	14.87	14.76	14.64
I 3947	5650	15.72	15.60	15.51	15.35	15.25	15.14
I 3949	7537	15.84	15.62	15.45	15.20	15.02	14.81
I 3955	7690	15.88	15.72	15.59	15.40	15.25	15.09
I 3963	6727	16.02	15.87	15.75	15.59	15.44	15.32
R 268	7850	16.59	16.43	15.30	16.10	15.94	15.75
R 230	5921	16.01	15.89	15.81	15.70	15.62	15.55
N 4871	7100	15.72	15.57	15.45	15.25	15.10	14.94
N 4873	5649	15.94	15.78	15.62	15.41	15.23	15.04
R 26	6872	15.79	15.64	15.54	15.39	15.30	15.19
N 4874	7148	15.62	15.30	15.07	14.79	14.58	14.31
N 4875	7855	15.77	15.63	15.52	15.36	15.24	15.13
N 4895	8420	15.23	15.03	14.90	14.69	14.52	14.34
R 124	6978	15.95	15.80	15.69	15.52	15.39	15.24
			SBO, a GALAXIES				
N 4854	8062	15.99	15.83	15.70	15.49	15.33	15.16
R 219	5366	16.07	15.94	15.84	15.68	15.56	15.42
I 3960	(6584)	15.76	15.65	15.54	15.39	15.27	15.14
I 3973	4732	15.37	15.25	15.15	15.03	14.91	14.82
N 4872	6972	15.78	15.62	15.52	15.35	15.25	15.11
I 3998	9358	15.90	15.76	15.62	15.42	15.28	15.17
N 4883	7949	15.75	15.60	15.47	15.26	15.11	14.96
R 87	7394	16.27	16.16	16.08	15.94	15.85	15.77
R 91	6179	16.34	16.25	16.19	16.07	15.98	15.92
I 4042	6243	15.72	15.54	15.40	15.22	15.07	14.93
R 113	8056	16.23	16.09	15.99	15.82	15.72	15.61

FIGURE 3

Equivalent V-m diagrams for the Coma and Virgo Clusters. E galaxies are shown as filled circles, SO as open circles, SBO or SBa as plus signs, and later Virgo Cluster spirals with S symbols. Both clusters show an identical pattern of redshift as a function of magnitude with the Coma Cluster displaced twoard the higher redshift domain. The break from the rp-branch into the transitional loop in both clusters appears to differ systematically as shown for SO and SBO or E galaxies.

region is represented with primarily SO and SBO galaxies. These galaxies tend to fall below the high redshift end of the rp branches and appear to be directly equivalent to the S subsystem objects in the Virgo Cluster further supporting the concept that the difference in mean redshift of the Virgo E and S subsystems does not arise because of different cluster membership or distances. The Coma Cluster core contains only one n-branch galaxy, NGC 4889, lying at the end of the branch defined by the Virgo Cluster bright elliptical galaxies. NGC 4874, the second luminous extended galaxy in the Coma Cluster may represent a further extension of the n-branch as shown. As discussed in the Virgo Cluster section, small aperture measurements of the diffuse objects near the end of the n-branch tend to drop back toward the rp-branch, but by means of integrated or large aperture photometry they are recognized to be n-branch galaxies.

THE HUBBLE CONSTANT

Given V-m diagrams for a series of aperture sizes in both the Virgo and Coma Clusters, a fitting process may be followed to derive a differential distance modulus for the clusters. Starting from approximately equivalent diagrams, such as the two shown in Figure 3, the redshift difference between the clusters is determined primarily by matching the low redshift end of the T-region and the break where the rp-branch joins the T-region. This differential between Coma and Virgo is 5060 ±50 (estimated error).

The second step in fitting consists of taking the V-m diagram for one specific aperture size in one cluster, aligning it with the V-m diagram for each of several aperture sizes in the second cluster by shifting by the cluster redshift difference and determining the differential magnitude between the diagrams. Corrections for K dimming and galactic absorption are applied before the fit is determined. The measured differential magnitude is then

plotted against aperture size for the second cluster as shown with the solid line in Figure 4, where Virgo Cluster 38.7 arc second photometry has been compared with the Coma Cluster for six aperture sizes.

A second line is generated in the differential magnitude-aperture diagram by the following reasoning. If two identical galaxies or sets of galaxies lie at distances d_1 and d_2, the magnitude differential between equivalent emitting volumes of the galaxies is given by the inverse square law as

$$\Delta m = 2.5 \log \left(\frac{d_2}{d_1} \right)^2 . \qquad (2)$$

This actual differential will be observed only if the observing apertures have a diameter ratio equal to the inverse of the distance ratio. Thus, for each aperture pair compared in the V-m fitting process, one may calculate a Δm value

$$\Delta m = 2.5 \log \left(\frac{D_1}{D_2} \right)^2 , \qquad (3)$$

which the galaxies must have if the aperture ratio is actually equal to the distance ratio. The dashed line in Figure 4 is drawn through the calculated Δm for each aperture pair used in fitting. The intersection of the two lines occurs at Δm equal to the apparent differential distance modulus of the clusters and at the aperture value for the Coma Cluster corresponding to the diameter of the emitting volume defined by the aperture used on the Virgo Cluster. In Figure 4 for 38.7 arc second Virgo Cluster data, the differential distance modulus is 3.45. In Figure 5 the same fit is illustrated for 25.8 and 64.5 arc second Virgo Cluster photometry. All fitting parameters and results are summarized in Table III. The three determinations are in good agreement and yield a final apparent differential distance modulus of 3.47 ±0.05 (estimated error) corresponding to an apparent distance ratio of 4.94 ±0.11. Corrections

FIGURE 4

Magnitude differences between the Coma and Virgo Clusters for 38.7 arc second Virgo photometry and six Coma Cluster aperture sizes. The intersection of the observed difference line with the line predicted by the aperture ratio determines the differential distance modulus between the clusters.

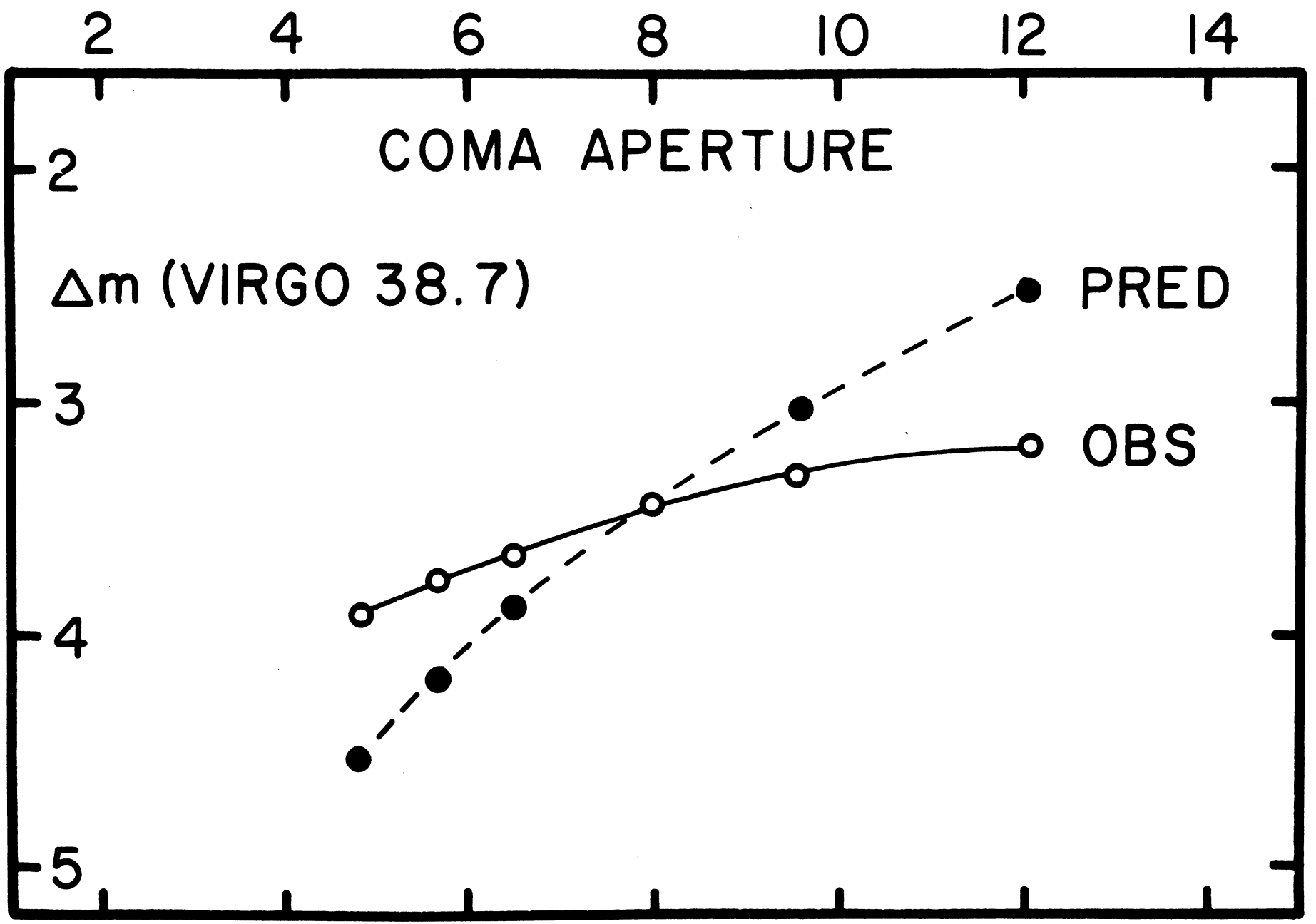
2
4
6
8
10
12
14
COMA APERTURE
2
Δm (VIRGO 38.7)
PRED
3
OBS
4
5

FIGURE 5

Magnitude differences between the Coma and Virgo Clusters for 25.8 and 64.5 arc second Virgo photometry and six Coma Cluster aperture sizes.

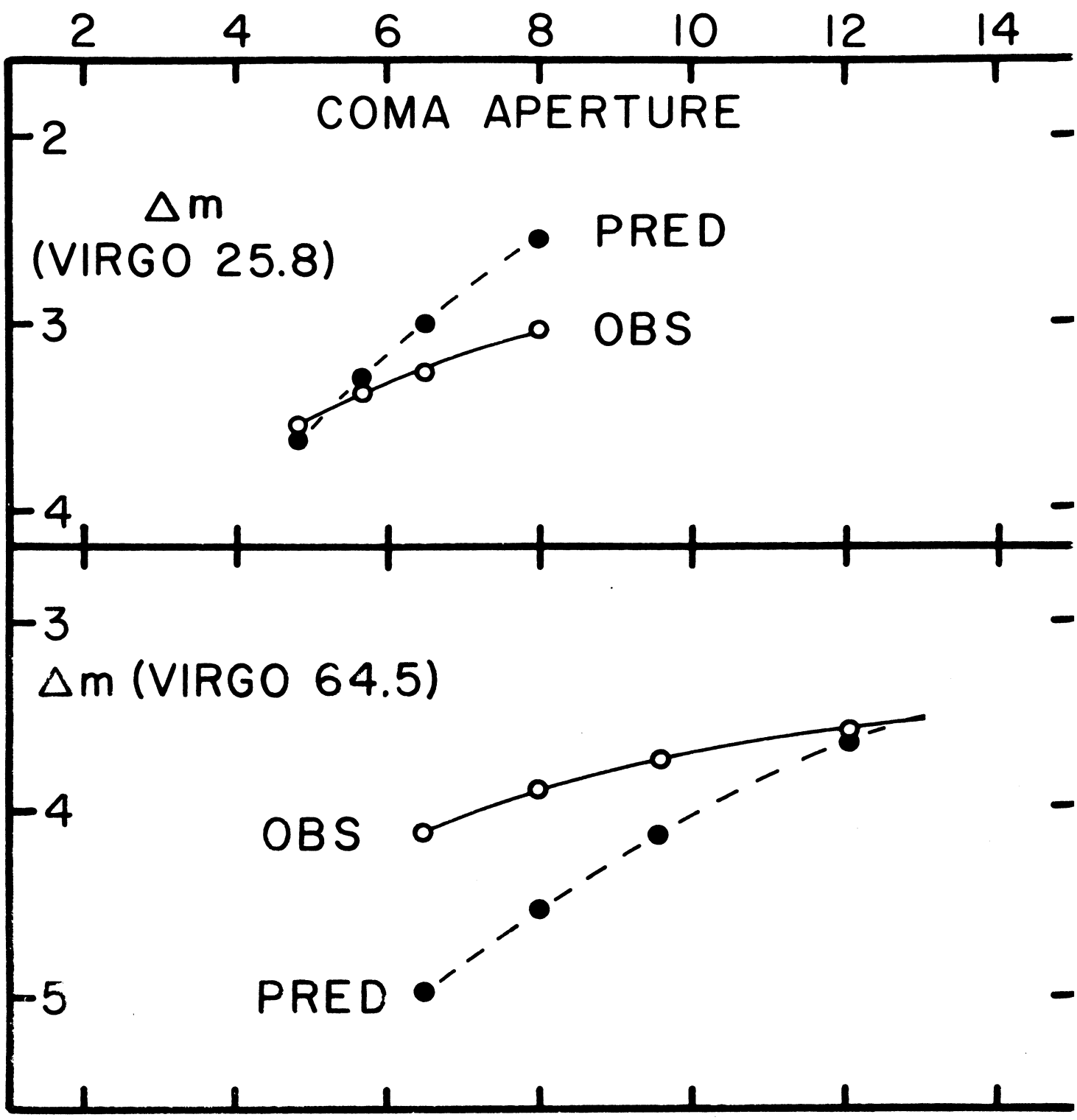
2
4
6
8
10
12
14
COMA APERTURE
2
Δm
(VIRGO 25.8)
PRED
3
OBS
4
3
Δm (VIRGO 64.5)
4
OBS
PRED
5

TABLE III -- COMA-VIRGO MAGNITUDE DIFFERENCES

APERTURE (VIRGO)		APERTURE (COMA) 4.80	5.64	6.47	7.96	9.57	12.05	INTERCEPT	WEIGHT
25.8	Δm(obs)	3.55	3.38	3.26	3.04			3.455	2
	Δm(pred)	3.65	3.30	3.00	2.55				
38.7	Δm(obs)	3.90	3.76	3.65	3.44	3.30	3.18	3.455	4
	Δm(pred)	4.53	4.18	3.88	3.43	3.03	2.53		
64.5	Δm(obs)			4.12	3.89	3.74	3.58	3.56	1
	Δm(pred)			4.99	4.54	4.14	3.64		

Note: Δm(obs) is corrected for differential absorption and K effect.

for differential K dimming and differential galactic absorption totaling 0.04 magnitudes were applied in the fitting process by shifting the observed Δm curve by 0.04 magnitudes. K corrections have been taken from Oke and Sandage (1968) for the mean cluster redshifts while differential absorption has been derived from a conventional cosecant b law assuming a galactic pole absorption of 0.18. Both corrections are very small.

If we now assume that a uniform Hubble expansion applies over the distance interval from the Virgo to Coma Clusters we can write

$$\frac{V_H(\text{Virgo})}{V_H(\text{Coma})} = \frac{d(\text{Virgo})}{d(\text{Coma})}. \tag{4}$$

We further know from the first step in the V-m fitting process that

$$V_H(\text{Coma}) = V_H(\text{Virgo}) + 5060. \tag{5}$$

Combining the equations yields values of the Hubble velocities of the clusters independent of the actual distribution of points in the V-m diagrams for either cluster. The results for the two clusters are

$$V_H(\text{Virgo}) = 1284 \pm 45, \tag{6}$$

$$V_H(\text{Coma}) = 6344 \pm 70. \tag{7}$$

These values may be compared with actual mean redshifts in the clusters of 1136 for Virgo (Humason, Mayall, and Sandage; 1956) or 950 for the Virgo E cloud alone (deVaucouleurs, 1961b) and 6891 for Coma (Rood, et. al., 1971). If we assume a true distance modulus for the Virgo Cluster of 30.85 (distance 14.80 Mpc) as given by Sandage (1968), we find a Hubble constant of

$$H = 86.8 \pm 3.0, \tag{8}$$

which is higher than the value given most recently by Sandage (1968) but well

within the random uncertainty of the determination. The random error in this determination of H is considerably smaller than given by Sandage (1968) and arises directly from the fitting uncertainty. It appears that random error uncertainty in H may be reduced to below the five percent level.

Systematic errors provide by far the major uncertainty in H. Uncertainty in the Virgo Cluster modulus is a primary problem as indicated previously by Sandage (1968). A small effect arises from uncertainty in the differential absorption. K corrections are now well determined and are not a significant source of error at the distances here considered. Anisotropy in the local Hubble flow, if present, slightly perturbs the solution for the cluster Hubble velocities. It is possible, however, that the Hubble flow is actually quite uniform and the local anisotropy is a consequence of the distribution of differential redshift components not related to motion of the mass centers of galaxies. In any case, Sandage (1968) has shown that anisotropy at the distance of the Virgo Cluster is small. Definitive study of individual cluster random motions and irregularity in the Hubble flow will require study of additional clusters to determine the uniformity of H values derived.

Stellar evolutionary systematic corrections in magnitudes of galaxies are not significant at the distance of the Coma Cluster, however, systematic evolutionary corrections to both redshift and magnitudes may be of importance for galaxian evolution itself. If the V-m relationship is actually an evolutionary track of galaxy nuclei, one cannot rule out systematic deviations in both absolute magnitude or redshift between the clusters, especially since the distribution of galaxies in the Virgo and Coma Clusters on the n and rp branches is different. No estimate of this effect can be made until additional clusters have been studied. In particular, clusters with both similar and different V-m diagrams must be intercompared. Preliminary studies of other

clusters show a considerable degree of uniformity so that the dominant uncertainty in H probably remains as the Virgo Cluster modulus.

APPLICATIONS AND THE EVOLUTIONARY CONCEPT

Figure 6 is a composite V-m diagram for 25.8 arc second Virgo Cluster core photometry and 5.22 arc second interpolated Coma Cluster core photometry. A scale of absolute magnitude is indicated based upon an apparent Virgo cluster modulus of 31.1 as given by Sandage (1968). The redshift coordinate, δV, is shown differentially with respect to the Hubble velocity as previously derived. Zero differential redshift appears to correspond closely with the end or bend in the n-branch and the beginning of the transition region on the rp-branch.

In the second paper in this series (EGN II, in preparation), the V-m correlation is extended into the domain of integrated galaxy magnitudes. Because of atmospheric limitations on small aperture nuclear region photometry, it is in integrated form that studies of distant clusters must be made. The basic correlation has been found to be present in all clusters or groups where a sufficient number of redshifts and magnitudes are available to permit an investigation. The scatter observed in integrated magnitude correlations is greater since a wide variety of outer structural variation is included in the photometry. In particular, secondary star formation, especially in spirals, may add luminosity and tend to mask the primary correlation of nuclear origin. Thus, at this time the primary correlation is defined by E and SO type galaxies only.

As successively smaller apertures are considered, the V-m correlation becomes more distinct and some galaxies which fall below or above the rp-branch at large apertures appear to converge toward it. The spread of luminosity within the brighter galaxies in general becomes less as was originally noted

FIGURE 6

Composite V-m diagram for 25.8 arc second Virgo Cluster photometry and 5.22 arc second Coma Cluster photometry. The differential redshift is shown with respect to the Hubble velocities derived for the clusters. The absolute magnitude scale is based upon an apparent Virgo Cluster modulus of 31.1.

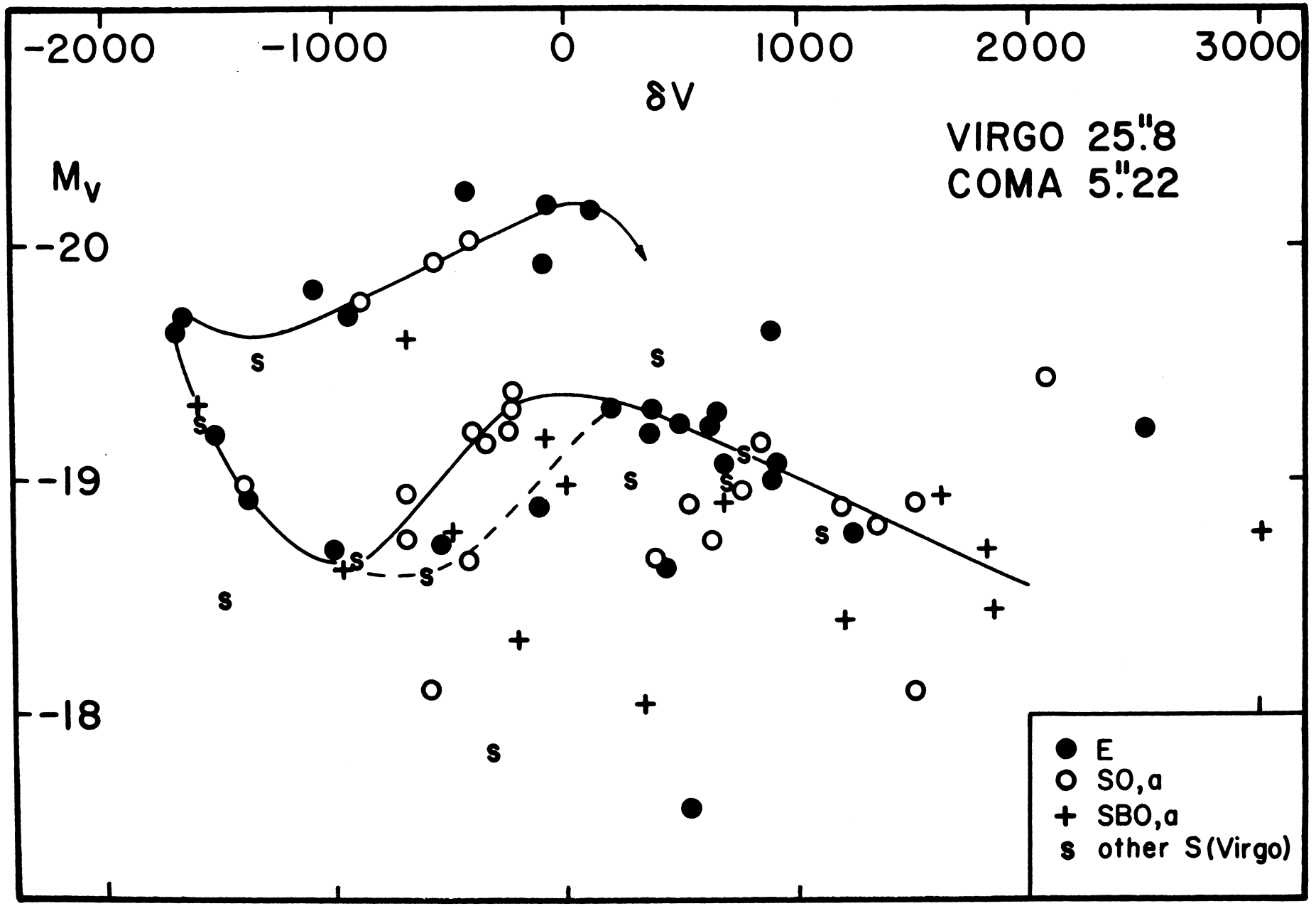
-2000
-1000
0
1000
2000
3000
δV
VIRGO 25.''8
COMA 5.''22
M_V
-20
-19
-18
E
SO,a
SBO,a
s other S(Virgo)

by Tifft (1963). This is apparently due to the tendency for the n-branch to flatten out at small apertures. At very small apertures in the Virgo Cluster, a new source of scatter appears in the m and conceivably the V coordinate due to nuclear activity which is manifest optically by abnormally red or blue nuclei (Tifft, 1969). These nuclear photometric anomalies have been shown to correlate with small nuclear radio sources (Tifft, 1970) and may represent active stages in a nuclear evolutionary process.

The rp-branch may be an upper envelope rather than a distinct branch like the n-branch. Insufficient data on redshifts of faint galaxies is available to answer this question. There is evidence from the luminosity function in the Coma Cluster that the frequency of elliptical galaxies peaks at one or more distinct magnitudes, the primary bright peak corresponding to the projection of the rp-branch. This is shown in Figure 7 where V(R = 4".80) photometry is plotted for all Come core E, SO, and SBO galaxies brighter than V(R = 4".80) = 17.5. For most galaxies fainter than V = 16.3, the correction from V(A) to V(R) has been approximated. The existance of peaks in the luminosity function of integrated magnitudes of galaxies has been reported by various authors (Rood, 1970; Abell, 1962). The main E galaxy peak appears distinctly for nuclear magnitudes. SO galaxies peak well below the primary rp E galaxy projection. Little redshift data are yet available on faint SO galaxies, however, there is a tendency in the available fainter SO or SBO galaxies to prefer higher redshifts and define an S region very similar to Virgo.

The peaks in the luminosity function of the Virgo and Coma Clusters may be enhanced by applying a magnitude correction as a function of redshift. Both the n and rp-branches, as defined by elliptical galaxies, slope at roughly 0.5 magnitudes per 1000 km redshift change for the Coma 5.22 arc second or Virgo 25.8 arc second photometry. Figure 8 shows the normal luminosity function

FIGURE 7

The V(4".80) nuclear magnitude luminosity function of E, SO, and SBO or SBa galaxies in the Coma Cluster core with V(4".80) $\leq$17.5. The primary peak in E galaxy frequency is a consequence of projection of the rp-branch in the V-m correlation. SO galaxies concentrate at a distinctly fainter magnitude where E galaxies are deficient.

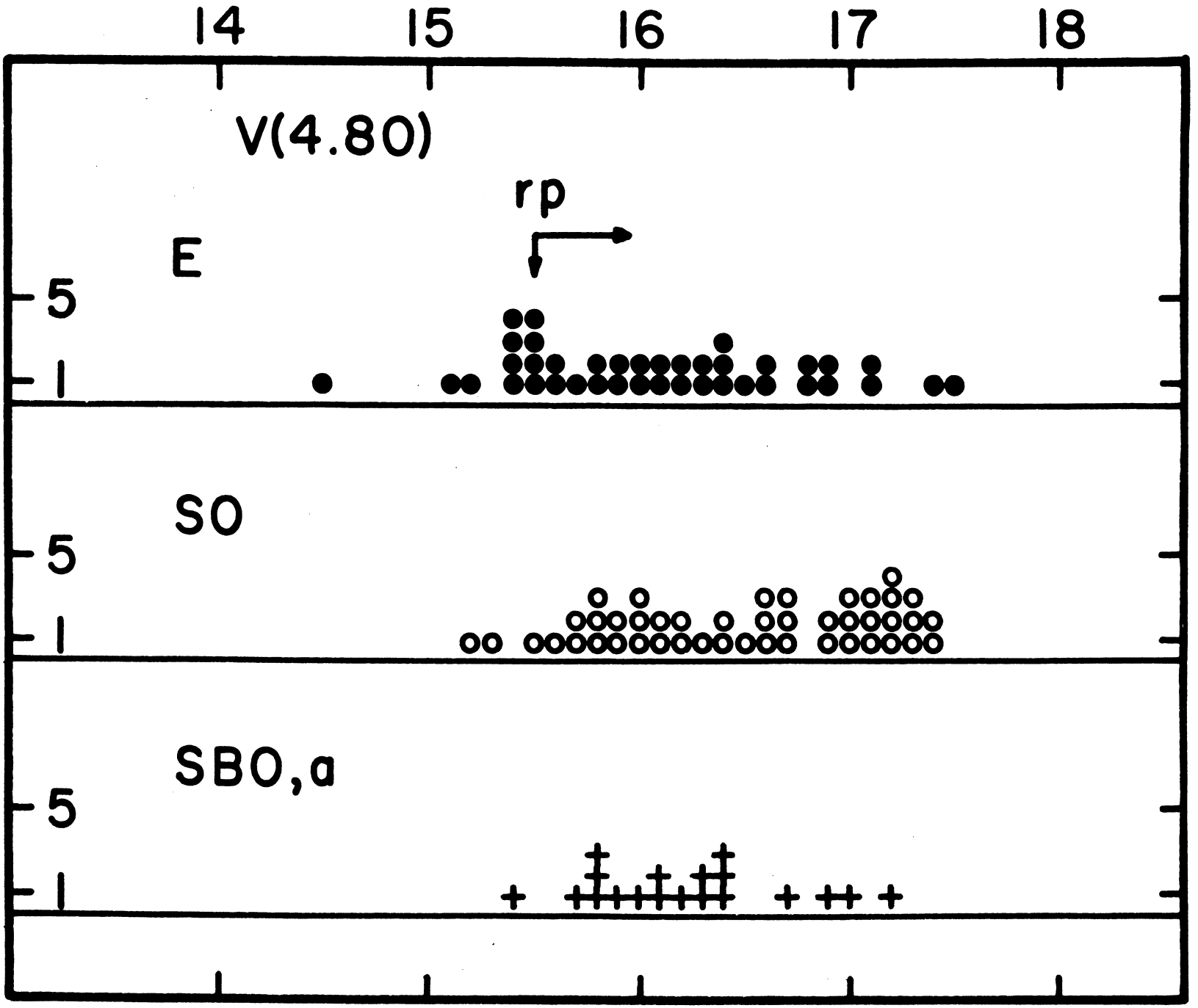
14
15
16
17
18
V(4.80)
rp
E
5
1
SO
5
1
SBO,a
5
1

FIGURE 8

The luminosity function for E(●), S0 or Sa (o), SB0 or SBa (+), and later spirals (S, Virgo only) which have redshift determinations. The Coma Cluster galaxies have been referred to the Virgo Cluster distance. On the left the normal luminosity function (LF) is shown while on the right a correction to the magnitude has been made based upon redshift to enhance the projections of the n and rp-branches in the V-m correlation (VTLF).

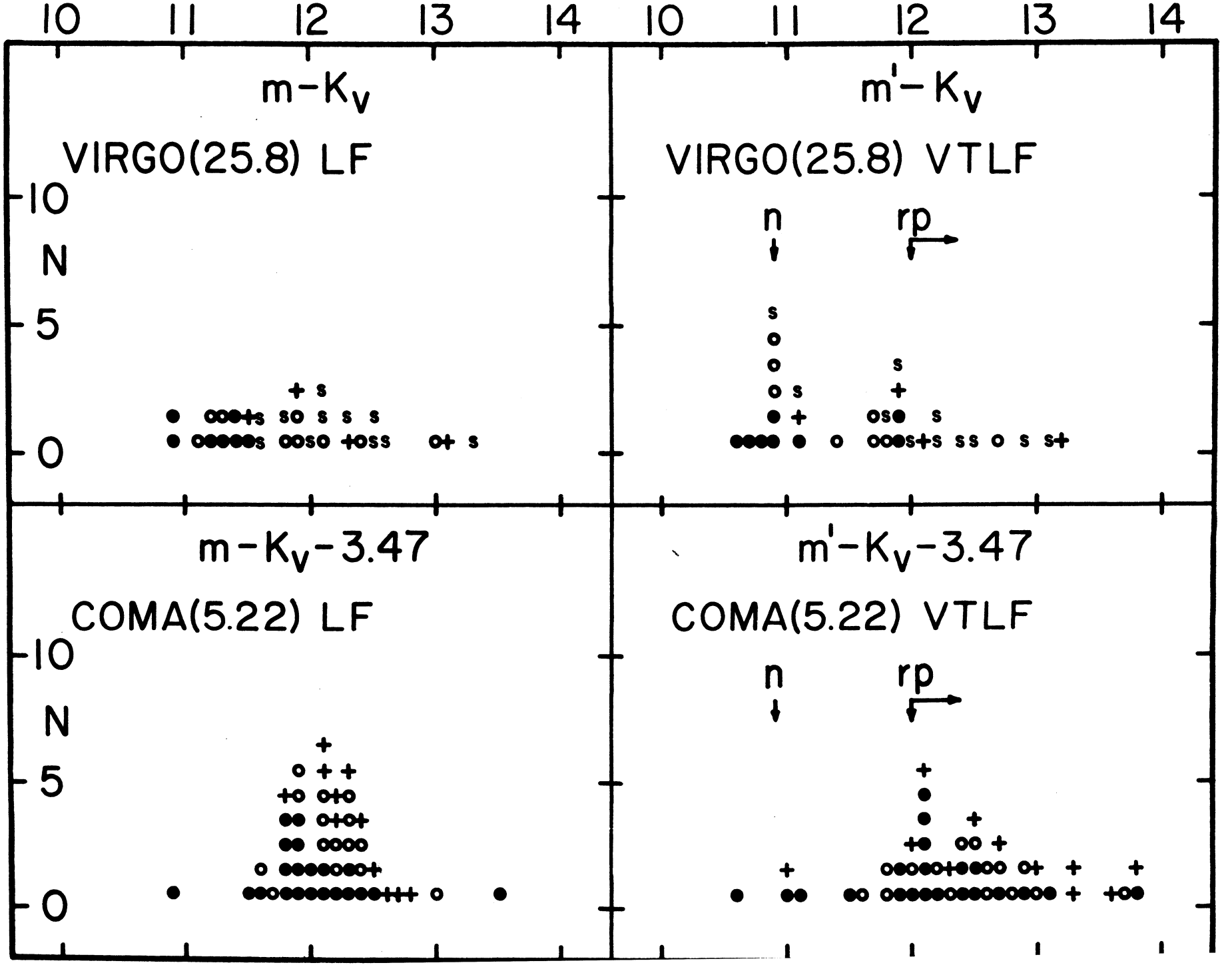
10
11
12
13
14
m-K_V
VIRGO(25.8) LF
N
10
5
0
m'-K_V
VIRGO(25.8) VTLF
n
rp
m-K_V-3.47
COMA(5.22) LF
m'-K_V-3.47
COMA(5.22) VTLF

(LF) and the velocity-transformed-luminosity-function (VTLF) for galaxies with known redshifts in the two clusters. The revised magnitudes were computed according to the relationship

$$m' = m + 0.5 \frac{\delta V}{1000}, \tag{8}$$

where δV is the differential redshift from the Hubble velocity. The peaks of galaxy frequency are enhanced and the Coma and Virgo luminosity functions show a much more obvious resemblance to each other. A simple VTLF is not possible for integrated magnitudes since the n-branch is much steeper than the rp-branch for integrated magnitudes.

The luminosity function analysis suggests that the rp-branch does have a deficiency of E galaxies below as well as above it but further study is required to determine if SO objects blur the gap or extend the branch. It is known in the Virgo Cluster that "lenticular" (SO) galaxies, as well as spirals, show systematically higher redshifts than ellipticals (deVaucouleurs and deVaucouleurs, 1963). Another interesting viewpoint on the distribution of fainter galaxies in the Coma Cluster is obtained by plotting the 4.80 arc second magnitudes against the ellipticity indices given by Rood and Baum (1967). This is shown in Figure 9 and illustrates well the role of the lenticular SO types in the gap below the brighter ellipticals.

In much of what has proceeded in this paper, the underlying cause of the V-m correlation is not critical. The cluster fitting process may be useful in distance and H determination and through multiple H determinations may yield data on the uniformity of the Hubble flow and possibly q, the deceleration parameter. To proceed far in this direction, however, the question of the source of the V-m correlation becomes critical since evolutionary factors could become large.

FIGURE 9

V(4".80) nuclear magnitude in the Coma Cluster as a function of ellipticity. Symbols are E (•), SO (o), and SBO or SBa (+). The sample is complete to 17.6 magnitude for the Coma Cluster core. The lenticular SO galaxies concentrate well below the concentration of E galaxies.

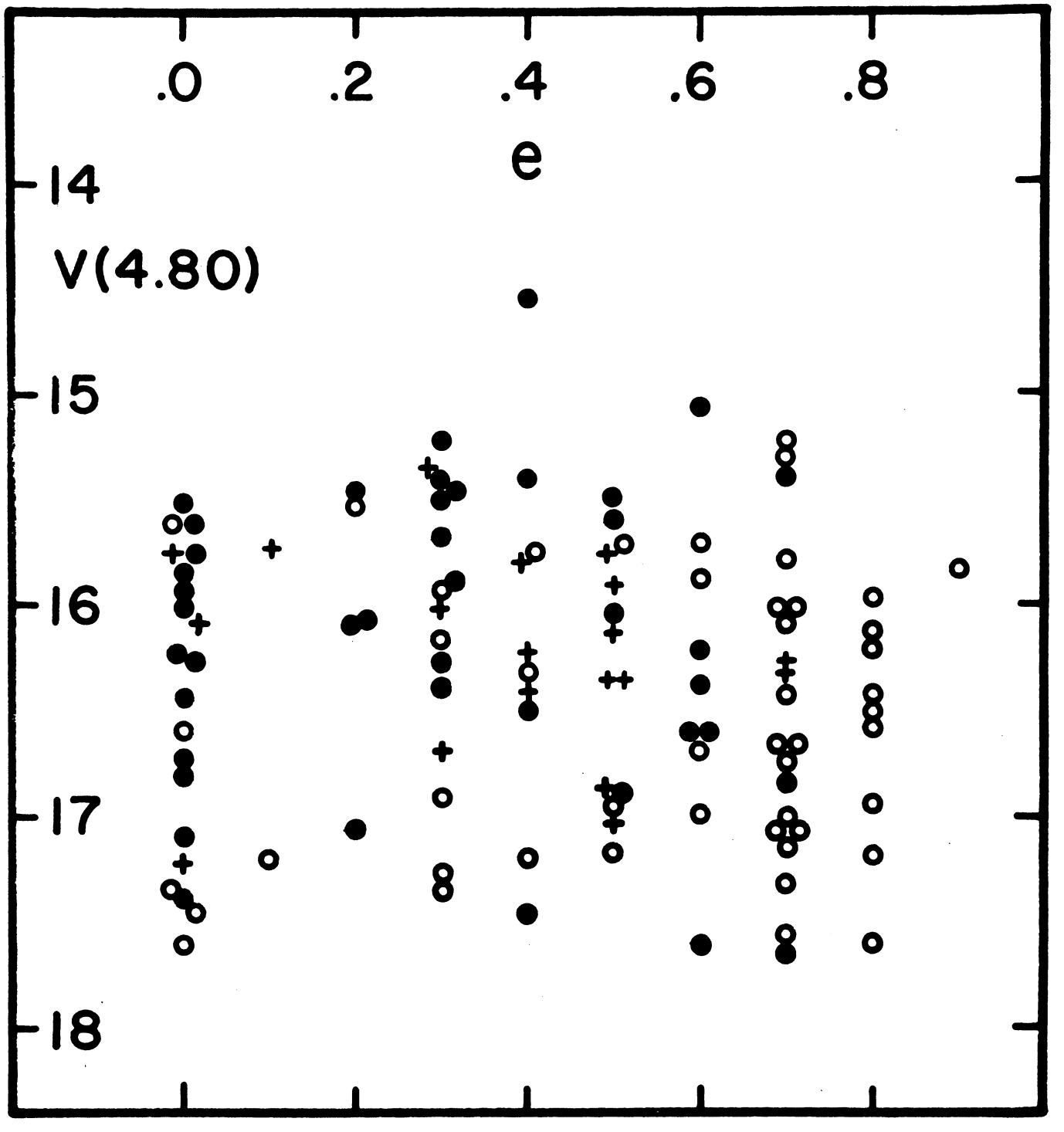
.0
.2
.4
.6
.8
e
14
V(4.80)
15
16
17
18

The present interpretation of the V-m correlation, Tifft (1970), views the rp-n track in the diagram as an evolutionary track along which galaxies move in time. The track is a locus of different galaxies seen at the same time. Parameters such as mass and angular velocity may vary smoothly along the observed sequence. The close fit obtained between the Coma and Virgo Clusters, despite the fact that the Coma Cluster appears to be shifted systematically along the track, suggests that individual tracks may not deviate widely from the V-m mean pattern. One particular redshift, the Hubble velocity V_H, is interpreted as the systematic true Doppler motion of the entire cluster of galaxies. The differential redshift, δV, with respect to the Hubble velocity is ascribed to some other cause and is discussed in the next section. The negative differential redshift is considered most likely to represent radial mass flow outward from a nuclear region where the gravitational potential has been or is being relatively rapidly reduced by mass loss through a mechanism such as gravitational radiation or mass point ejection. The positive differential redshift effect is considered most likely to be a gravitational redshift.

Whatever the detailed mechanism producing the differential redshift, it does not appear that a model of mass center motion distribution is possible because of the marked asymmetries in the redshift distribution. Actual mass center motion dispersion within clusters must, therefore, be found <u>within</u> the dispersion of points about the basic V-m correlation track itself. Allowing for measuring uncertainties in redshifts and magnitudes, as well as magnitude scatter due to effects discussed in the section on fitting of V-m diagrams together and cluster depth effects for Virgo, any true velocity dispersion appears to be masked but is not likely to much exceed one hundred kilometers per second. Since a cluster mass calculated from the Virial Theorem varies as the square of the velocity dispersion, a cluster mass reduction of one to two

orders of magnitudes from published Virial masses is implied. This can reduce M/L values derived from clusters to the order of 10 and clusters can be inherently stable.

Sandage (1970) has remarked on the uniformity of the luminosity and small dispersion in the redshifts of the first ranked cluster galaxy, especially if selected by being a radio galaxy. This characteristic will be a natural consequence of the V-m pattern where all real velocity dispersion is small and luminosity is fixed in an evolutionary scheme and not as a random variable. The strong radio source object, NGC 4486, in the Virgo Cluster occupies the bright tip of the n-branch as do the strong extended radio sources in all other clusters yet investigated, some of which are discussed in EGN II (in preparation). If the low velocity dispersion of the most luminous object was a consequence of equipartation of energy with the most massive object being nearly stationary, then those galaxies ranking next in luminosity should scatter in velocity to both higher and lower redshifts. In fact, the Virgo V-m diagram shows that the next ranked E galaxies lie at lower redshifts and define the n-branch structure.

It was earlier suggested that the V-m diagram differences between the Coma and Virgo Clusters could represent different cluster ages, hence, different progress along the track. Two factors could produce such a shift--dispersion in actual age of cluster formation or emergence into visibility and light travel time looking outward, hence, earlier in time. The light travel lookback time differential between the Coma and Virgo Clusters is only a few times 10^8 years which is of the same order as the rotation period of a galaxy, hence, not time enough for major mass flow and dissipation to occur as

proposed herein as one major mechanism in galaxy evolution. Furthermore, the NGC 545 Cluster at nearly the same distance as Coma shows a V-m pattern very similar to Virgo (EGN II, in preparation). The relatively nearby Ursa Major Cloud appears, if anything, to be slightly older than the Virgo Cluster. Finally, the observation of distant radio galaxies of the type apparently associated with the n-branch locally may imply that clusters at considerable lookback times have had time to evolve into the n-branch. In general, the observations viewed in the context of an evolutionary scheme for clusters favor a distinct dispersion in cluster ages. Detailed pursuit of this concept could provide a powerful tool for distinguishing between steady state and singular origin cosmologies.

If one assumes a cosmology with a singular universal origin combined with evolving clusters, some commentary on q is possible. With increasing distance and lookback time, clusters will be seen at earlier and earlier stages. If the apparent age pattern discussed above is at all correct, the younger (distant) clusters will trend back toward the higher redshift end of the rp-branch and the mean redshift may overestimate the true Hubble velocity or distance. It is difficult to estimate how luminosity would vary back along the rp-branch, but by choosing the "appropriate" pattern, almost any m, log cz, plot could be predicted. If the concept of galaxy evolution by mass outflow is considered, one can argue that at earlier times the galaxies were more massive and perhaps more luminous as a result. Thus, not only might log z be too large but m might be too bright. Such effects may give a mechanism which can produce a negative value for q.

THE DIFFERENTIAL REDSHIFT

A possible interpretation of the negative V portion of the V-m diagram has been given in terms of radial mass outflow under the influence of an

evolving gravitational potential (Tifft, 1970). Arguments favoring such a model include the following. Virgo Cluster galaxies which are extreme examples of negative δV are NGC 4406 and NGC 4438 which have $\delta V = -1651$ and -1389 respectively. Both of these galaxies show extended halo or filament structure which could be produced by rapid outflow of material. The outflow could be forceful ejection, however, a potentially simpler mechanism is to reduce the central mass potential through gravitational radiation and an outflow will automatically result. No acceleration mechanism is required operating on concentrated masses. The observation of excessive gravitational radiation from the direction of the Galactic nucleus (Weber, 1969) suggests that major rapid mass loss in galactic nuclei must be considered. Further evidence for nuclear mass outflow is provided by the spectrographic observations of Rogers and Freeman (1970) in the nucleus of NGC 4569. This Virgo spiral type galaxy also lies at extreme negative δV for the cluster. The absorption, hence stellar component, velocities in the nucleus and disc can be fitted with a rotation plus very rapid expansion. Expansion velocities for the gas component in galaxies are known in numerous cases, however, mechanisms to accelerate gas are quite possible so gas expansion need not agree with motion of the stellar component.

Another major feature of some galaxies which can be explained in terms of mass flow outward from galaxies is intergalactic bridges and related structure. In the absence of nearby major gravitational masses, the outflow of material will presumably take the form of a general extended halo or a series of shell-like structures according to whether the potential changed smoothly or stepwise. Such galaxies are known--NGC 4486 with the extensive halo (Arp and Bertola, 1969) and several additional galaxies studied more recently (Arp and Bertola, 1970). NGC 474, NGC 509, and others in the Atlas of Galaxies by Arp (1969) are examples showing shell-like structures.

In the presence of a nearby massive object, mass released from a galaxy could be directed to produce the bridge phenomena. The bridges are not made up of diffuse gas since, except in specific condensations, they show an absorption spectrum (Zwicky and Humason, 1969). They must represent a flow phenomena of massive objects, presumably stars. It is also well known that many bridges do not actually connect to an adjacent object or may even lead toward no visible object. Non-connection would be expected frequently for mass outflow being directed by a distant potential. Methods of producing a massive potential with no visible object are possible if the mass resides within the Schwarzschild radius. As recently reviewed by Harrison (1970) emergence of massive objects through the Schwarzschild radius may represent the actual origin of galaxies; the V-m type track could be the evolutionary track of such a process with mass loss by gravitational radiation and outflow as primary evolutionary consequences. As a final product of outflow from galaxies in a cluster, one should see a general intergalactic haze within clusters. DeVaucouleurs and deVaucouleurs (1970) have measured this haze in the Coma Clusters. The recent work by Arp and Bertola (1970) further shows its presence and source. It is very difficult to envisage forming stars in intergalactic space, however, the outflow concept will require their presence.

Other observed conditions which could find their explanation in mass outflow in a decreasing potential include variation of ellipticity of galaxies with radius and rotation of directions between inner and outer elliptical isophotes. Bar, ring, and spiral patterns in galaxies are structures quite possibly originating in an evolving potential field, as are the stellar relaxation states observed in galactic halos. The expansion of a rotating system with loss of objects at the outside should also give a mechanism for angular momentum evolution. Non-steady state conditions implied by an outflow

model should permit correlation of internal velocity dispersion from spectral lines with location in the V-m diagram. There is evidence (Tifft, 1970) that dispersion increases along the n-branch. The determination of elliptical galaxy masses from velocity dispersion observations may be questioned.

If the evolutionary concept of galaxies is correct and a galaxy evolves through the V-m diagram, it will eventually reach the luminous n-branch. Since galaxies do not collect there, it would appear that galaxies may evolve rapidly down in luminosity, possibly ultimately leaving a form of dwarf galaxy remnant. Galaxies in this terminal state would have to show an extended terminal halo, no prominent bright nucleus, and a velocity close to the Hubble velocity since no major mechanism would remain to perturb the redshift. This is the observed nature of the tip of the n-branch.

On the basis of the density of points along the V-m track an estimate of evolutionary rate is possible. The transitional zone appears to be relatively sparce in membership compared with both the n and rp branches. A rough estimate of the duration of the transition period would be a few galactic revolutions, roughly 5×10^8 years. The time spent on the rp or n branches is probably at least several times this figure but probably not an order of magnitude greater. The total time to evolve through the entire pattern may not be far from the Hubble time.

To produce positive differential redshifts, one might invoke infall of material, however, the time scale for infall collapse would presumably be too short to fit the observed rp-branch pattern and a gravitational redshift is suggested instead. Zwicky (1966) has reported a possible nuclear gravitational redshift for an elliptical galaxy in the Coma Cluster. The nucleus reportedly has a redshift much higher than the envelope of the galaxy. The nuclei of rp-branch galaxies are apparently sharp and compact (Tifft, 1970) which would

be expected in a massive compact core capable of producing a gravitational redshift. Considering the possible origin of galaxies from massive cores expanding into the visible universe as discussed by Harrison (1970) the earlier stages will necessarily show a strong redshift. Many of the complex problems in galactic properties, relaxation, early star formation, element synthesis, etc., can apparently be explained by expanding individual cores as well as, if not better than, an expanding near uniform universe with later galaxy collapse. This is also true of the microwave background which could be an integral over the individual core expansions.

ACKNOWLEDGEMENTS

The author wishes to especially acknowledge Dr. Herbert J. Rood for permission to use and reproduce portions of unpublished photometry of Coma Cluster galaxies.

REFERENCES

Abell, G. O. 1962, Problems of Extra-Galactic Research, ed. G. C. McVittie (New York: Macmillan Co.) 213-238.

Arp, H. 1966, Atlas of Peculiar Galaxies, Mt. Wilson & Palomar Obs., Carnegie Inst. of Washington and California Inst. of Tech.

Arp, H. and Bertola, F. 1969, Astrophys. Lett. 4, 23.

Arp, H. and Bertola, F. 1971, Ap. J. 163, 195.

Harrison, E. R. 1970, M. N. R. A. S. 148, 119.

Holmberg, E. 1961, A. J. 66, 620.

Humason, M. L., Mayall, N. U. and Sandage, A. R. 1956, A. J. 61, 97.

Kowal, C. T. 1969, P. A. S. P. 81, 608.

Oke, J. B. and Sandage, A. R. 1968, Ap. J. 154, 21.

Rodgers, A. W. and Freeman, K. C. 1970, Ap. J. 161, part 2, L109.

Rood, H. J. 1969, Ap. J. 158, 657.

Rood, H. J. and Baum, W. A. 1967, A. J. 72, 398.

Rood, H. J. and Baum, W. A. 1968, A. J. 73, 442.

Rood, H. J., Page, T. L., Kintner, E. C. and King, I. R. 1971 (in preparation).

Sandage, A. 1961, The Hubble Atlas of Galaxies, Publication 618, Carnegie Inst. of Washington.

Sandage, A. 1968, Ap. J. 152, part 2, L149.

Sandage, A. R. 1970, Physics Today 23, 34.

Tifft, W. G. 1963, A. J. 68, 302.

Tifft, W. G. 1969, A. J. 74, 354.

Tifft, W. G. 1970, Astrophys. Lett. 7, 7.

Tifft, W. G. 1970, IAU Symposium 44, Uppsala, Sweden (in press)

deVaucouleurs, G. 1961a, Ap. J. Supp. 5, No. 48, 233.

deVaucouleurs, G. 1961b, Ap. J. Supp. 6, No. 56, 213.

deVaucouleurs, G. and deVaucouleurs, A. 1964, Reference Catalogue of Bright Galaxies, Univ. of Texas Press, Austin, Texas.

deVaucouleurs, G. and deVaucouleurs, A. 1967, A. J. 72, 730.

deVaucouleurs, G. and deVaucouleurs, A. 1970, Astrophys. Lett. 5, 219.

Weber, J. 1969, Phys. Rev. Letters 22, 1320.

Zwicky, R. 1966, Report On Work Done In Astronomy 1965/66, California Inst. of Technology, 19 pages.

Zwicky, F. and Humason, M. L. 1960, Ap. J. 132, 627.